Mechanical Instabilities of Biological Tubes

Edouard Hannezo,[1] Jacques Prost,[1,2] and Jean-François Joanny[1]

[1]*Physicochimie Curie (Institut Curie/CNRS-UMR168/UPMC), Institut Curie, Centre de Recherche, 26 rue d'Ulm F-75248 Paris Cedex 05, France*

[2]*ESPCI, 10 rue Vauquelin, F-75231 Paris Cedex 05, France*

(Received 8 March 2012; published 3 July 2012)

We study theoretically the morphologies of biological tubes affected by various pathologies. When epithelial cells grow, the negative tension produced by their division provokes a buckling instability. Several shapes are investigated: varicose, dilated, sinuous, or sausagelike. They are all found in pathologies of tracheal, renal tubes, or arteries. The final shape depends crucially on the mechanical parameters of the tissues: Young's modulus, wall-to-lumen ratio, homeostatic pressure. We argue that since tissues must be in quasistatic mechanical equilibrium, abnormal shapes convey information as to what causes the pathology. We calculate a phase diagram of tubular instabilities which could be a helpful guide for investigating the underlying genetic regulation.

DOI: 10.1103/PhysRevLett.109.018101 PACS numbers: 87.19.R−, 87.17.Pq

Tubular shapes are found ubiquitously in living organisms, from worms to humans and are fundamental structures of many organs: they convey liquids, gases, or cells throughout the body. Typical examples are arteries, intestinal tubes, or renal excretory canals. The disruption of these tubes is at the origin of many pathologies, and although a large body of work has focused on the molecular mechanisms underlying each disease and each type of tube [1–5], little attention has been given to the biomechanical aspects of tube stability. Here, we present a general framework to describe the instabilities of cellular tubes and we discuss the possibility to infer the underlying causes of pathologies by studying the shapes of the abnormally deformed tubes. Indeed, tube instabilities are observed in many different organs but always seem to fall into a limited number of physiological categories: dilated, sinuous, or varicose tubes [2,6]. From a physicist's point of view, these shapes are reminiscent of classical fluid instabilities. Nevertheless, a key difference with passive systems is that pathological instabilities result from the internal activity of the tube. Cell division, or active fluid pumping, is often the motor of the instability. Thus, a mechanical description of the tube shapes could bear a lot of information on the underlying mechanisms of tube formation and instability.

In the past years, progress has been made in the mechanical description of tissues as dividing elastic media [7–9]. Stresses inside the growing tissues are essential to determine the final architecture of an organ and conversely, there are feedback mechanisms of form on growth. We apply these models, which have been usually used for bulk tissues, to cylindrical geometries. We consider a wide variety of epithelial tubes that all share key features. The tube is composed of a layer of dividing epithelial cells, which exert pressure on the surrounding medium, and an elastic basement membrane which provides mechanical stability. A softer connective tissue, which we model as an infinite, viscoelastic material, is surrounding the tube.

This simple description suggests a competition between several forces. The fluid-tube interface has a tension and can undergo a Rayleigh-Plateau-like instability [10], like a cylindrical fluid jet breaking into drops. However, the tube is elastic, and can resist deformation as discussed for passive lipid tubes [11]. We wish to add active effects: epithelial cells grow (sometimes at an uncontrolled rate), and the tube can buckle under the load induced by growth. Cell divisions are driving an increase of the surface area of the tube that can be described by a uniform negative surface tension. As noted in [7], large enough mechanical feedback leads to a spatially uniform growth. We make this assumption here, given the regularity of the patterns observed on tubes. Tubes can also dilate because of an excess uniform fluid pressure. We successively investigate the morphologies sketched on Fig. 1. The Young's modulus

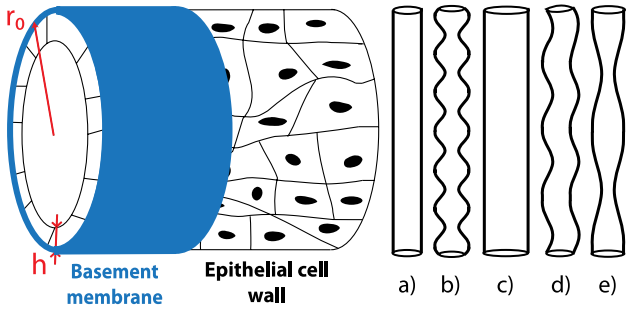

FIG. 1 (color online). Left: Sketch of our model for biological tubes. A single layer of epithelial cells rests on an elastic membrane (drawn on the left in light blue), surrounded by soft connective tissue (not drawn). Right: Different tube configurations: (a) reference, (b) varicose/pearling, (c) dilated, (d) sinuous (e) sausagelike. (b) and (e) have the same symmetry, but correspond to different instabilities, as described in the text.

E_t of biological tubes, such as arteries [12], is of the order of 10^4–10^6 Pa, which is stiff compared with the surrounding tissues. The reference state is a tube of infinite length and radius r_0. We first discuss a peristaltic perturbation (varicose) with cylindrical symmetry. The displacements in the direction z along the tube and the radial direction r are denoted by $u_z(z)$ and $u_r(z)$, respectively. The forces involved in the tube deformation can be derived from the following effective energy [13]:

$$\frac{\mathcal{E}_{\rm el}}{2\pi r_0} = \frac{E_t h}{2}\int (e_z^2 + e_\theta^2 + 2\nu e_z e_\theta) dz + \frac{K}{2}\int \left(\mathcal{C} - \frac{1}{r_0}\right)^2 dz, \quad (1)$$

where $\nu = 1/2$ is the Poisson ratio, and the strain components are defined as

$$e_\theta = \frac{u_r}{r_0} + \frac{1}{2}\left(\frac{u_r}{r_0}\right); \qquad e_z = u_z' + \frac{1}{2}(u_r'^2 + u_z'^2), \quad (2)$$

where the prime denotes a derivative with respect to z. The first term is the stretching elastic energy of the tube. We use the classical Föppl–von Kármán approximation [13], neglecting $u_z'^2$, but we keep the nonlinear term $(\frac{u_r}{r_0})^2$ that is relevant for large uniform dilations of the tube. The second term is the layer bending energy where $\mathcal{C}$ is the local curvature and $K = \frac{E_t h^3}{12(1-\nu^2)}$ is the bending modulus. A key difference with Ref. [14] is that we do not assume that the outer surface of the cylinder is fixed. The case of arteries is complicated by the presence of smooth muscles and anisotropy but as we wish to capture the essential physics, we restrain ourselves to this simple nonlinear and isotropic elastic theory. Tension and pressure forces drive the deformation and lead to an additional effective energy

$$\mathcal{E}_a = \int \{2\pi\gamma[r_0 + u_r(z)]\sqrt{1 + u_r'(z)^2} - \pi\Delta P[r_0 + u_r(z)]^2\} dz, \quad (3)$$

where γ is the effective tension, which contains a negative contribution due to cell division and which can therefore be positive or negative. ΔP is an excess pressure inside the tube. We first investigate a deformation of the tube to a radius $u_r(z) = r_0[R_0 - 1 + A\cos(kz)]$ which includes both a uniform dilation to a radius $R_0 r_0$ and a varicose deformation of amplitude $A \ll 1$ (see Supplemental Material [15] for details). We first discuss the effect of negative surface tension, assuming that the excess pressure is small, $\Delta P r_0 \ll |\gamma|(h/r_0)^2$. Compared with the classical Rayleigh-Plateau instability, the wavelength observed *in vivo* is small, close to the value of the tube radius [2,6,16]. We propose that this varicose instability is due to a buckling of the tube induced by the homeostatic pressure of the dividing epithelial cells. This hypothesis has biological grounds for hepatic arteries, since varicoses are associated with fibromuscular dysplasia [16–18] or polycystic disorders in renal canals [19].

In the following, we assume that the value of the tension is such that $\frac{h^2}{r_0^2} \ll \frac{|\gamma|}{E_t h} \ll 1$, which seems to be the case for reasonable values of the parameters: the tubes that we study are such that $\frac{h^2}{r_0^2} \approx 0.01$, and as discussed below, $\frac{|\gamma|}{E_t h} \approx 0.1$. The minimization of the energy with respect to R_0 leads to $R_0 = 1 + \frac{|\gamma|}{E_t h} \simeq 1$. In this limit, there is a bifurcation from tubular to varicose states for

$$|\gamma| > \gamma_p = E_t h \frac{h}{\sqrt{3} r_0} \quad (4)$$

at a wavelength $\lambda_p = 2\pi r_0[\frac{1}{1-\nu^2}(h/\sqrt{12}r_0)]^{1/2}$. The finite elasticity of the surrounding medium does not change these equations as long as its modulus E_s is such that $E_s r_0 \ll E_t h$, which is the case here. We have performed a numerical minimization of the total effective energy leading to the shape of a tube with a varicose instability shown in Fig. 2. For large arteries such as the common hepatic artery, the wall-to-lumen ratio is approximately $\frac{h}{r_0} = 0.1$, so that $\lambda_p \approx 1.23 r_0$. Strikingly, clinical studies [17] confirm that the wavelength of the pattern is proportional to the radius of the artery, with a very close coefficient of 1.3, in contradiction to analyses based on the Rayleigh-Plateau instability [20].

Away from the bifurcation point, there is a weak variation of the wavelength, which is compatible with the biological variability. This explains why the same range of wavelengths is always observed. Since the wavelength is of the order of the tube radius, we need not consider instabilities in the section plane of the tube, studied in Ref. [21] that becomes relevant for much thinner tube walls. The negative tension exerted by the cells is linked to the homeostatic pressure, $\gamma \approx -P_h h$ [22]. Pressure measurements for tumors or dysplasia give values in the range of $P_h = 10^4$ Pa [23]. Taking $E_t = 10^5$ Pa, the critical tension $\gamma_p \approx 7 \times 10^3 h$ is compatible with a buckling induced by the dividing cells.

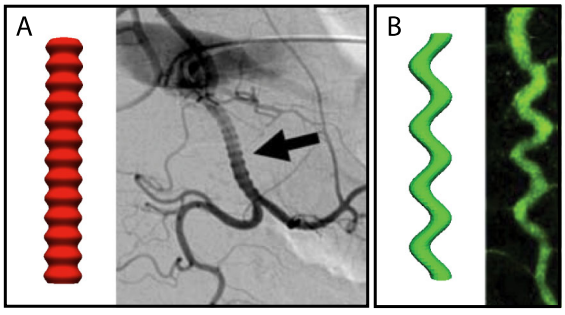

FIG. 2 (color online). Comparison between the shapes obtained from buckling theory and *in vivo* data. (a) A common hepatic artery displaying varicosities [16]. (b) A drosophila tracheal tube displaying sinuous mutation [32], $\lambda_s \approx 5 r_0$.

The tubular canals of the kidney in polycystic diseases lose their stability, giving rise to a variety of patterns: string of small pearls, large convolutions, or huge spheric cysts that can invade the entire organ [6,24]. Three mains factors [19] have been identified: increase in basement membrane compliance, uncontrolled division of the epithelial cells forming the tube wall, and disorders in ions pumps, causing excess water to be pumped in the canals. In our description, this relates respectively to a decrease in E_t, an increase in P_h, and an increase in ΔP. The excretory canal of *Caenorhabditis elegans* is often used as a model to study these diseases. Although the tube is different in nature [25] (a single, elongated cell invaginates to form a tube which spans its entire length), it can be described by similar equations: there is a bending energy associated to membrane deformation, a surrounding elastic medium prevents stretching, the tube can grow because of excess lipid transport (analogous to negative surface tension), and flows can be driven by hydrostatic pressure gradients. Thus, in order to incorporate the effect of pressure gradients, we now consider the opposite limit of dilated tubes, where the pressure dominates over tension effects, $\Delta P r_0 \gg |\gamma|(h/r_0)^2$. The equilibrium radius is such that the elastic deformation equilibrates the excess pressure:

$$R_0 = \left(1 + 2\frac{\Delta P}{E_t}\frac{r_0}{h}\right)^{1/2}. \quad (5)$$

The physical picture of the varicose instability is not modified greatly by considering the effect of an excess pressure. The threshold tension remains of the same order, and the characteristic undulation wavelength is slightly reduced: $\lambda_p = \lambda_p(\Delta P = 0)(1 + 5\Delta P r_0/3E_t h)^{-1/4}$.

We then turn to sinuous oscillations of the entire tube. The classical Euler buckling instability of an elastic column under compression occurs at a wavelength which is the system size, in the absence of any surrounding elastic medium. However, in an elastic medium, buckling occurs at a finite wavelength. We have shown recently that this instability can be invoked to describe the morphology of the intestine [26].

We call E_t and E_s the Young's moduli of the tube and surrounding elastic medium, respectively, keeping in mind that $E_t \gg E_s$. We denote the deformation of the tube by $h(z) = B\cos(kz)$. The curvature modulus of a hollow elastic tube is $K = \pi E_t r_0^3 h$, the force exerted by the growing tube is $f = 2\pi|\gamma|r_0$, and the elastic force exerted by the surrounding medium is proportional to the deformation with a coefficient $\alpha = \frac{2\pi}{1+\nu}\frac{E_s}{\log(\lambda/r_0)} \approx 2E_s$ (see Supplemental Material[15]). The threshold force of the sinuous instability is $f = 2\sqrt{K\alpha}$; thus, the critical tension for buckling is

$$|\gamma| > \gamma_s \approx 0.8\sqrt{r_0 h}\sqrt{E_s E_t}. \quad (6)$$

The wavelength of the instability is $\lambda_s = 2\pi r_0(\frac{h}{2r_0}\frac{E_t}{E_s})^{1/4}$. A rough estimate leads to $\lambda_s \approx 5$–$10 r_0$, in agreement with observations of degenerate excretory canals in *C. elegans* [6], or of the tracheal system in drosophila ([2] and Fig. 2).

We now compare sinuous deformations, which occur for cell tensions larger than γ_s given by Eq. (6), with varicose deformations with a threshold γ_p given by Eq. (4). The preferred morphology depends on the value of the elastic ratio $r = \frac{E_s r_0^3}{E_t h^3}$. If the substrate is very soft or the tube is very hard, the sinuous morphology is expected, since in that case, it requires a smaller tension. Conversely, if $\frac{h}{r_0}$ is very small, the varicose instability is expected. Physically, this is due to the fact that a tube with a larger radius costs more energy to bend than a tube with larger thickness: its curvature modulus varies as the cube of the radius and as the first power of thickness. For a typical tube, $\frac{h}{r_0} = 0.1$, and $E_t = 10^5$ Pa, the critical substrate rigidity separating both morphologies is $E_s = 10^2$ Pa. This analysis is important since a loss of tubular rigidity is one of the causes of cystic diseases. The situation is much more complex if the substrate is viscoelastic. Over long time scales, sinuous deformations are always expected, but can be kinetically constrained. A detailed discussion goes beyond the scope of this Letter [27].

In the region where both instabilities can be observed, it is necessary to compare the energies of the two morphologies. The results are displayed on a stability diagram in Fig. 3. We plot in thick green the transition line between the two instabilities, in the vicinity of the critical point.

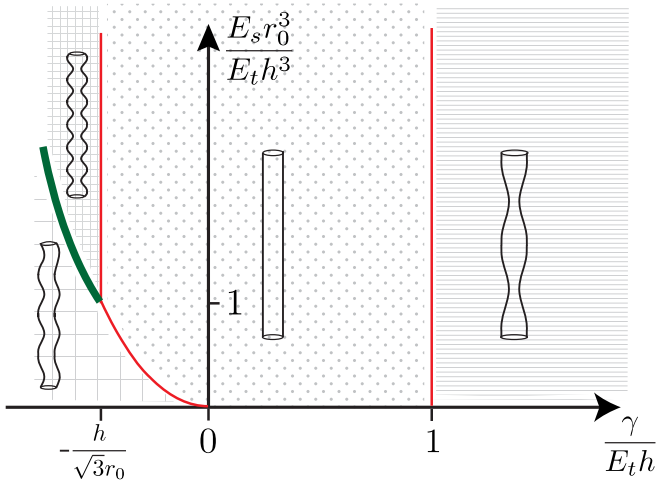

FIG. 3 (color online). Stability diagram of all possible configurations of a tube, depending on the relevant parameters. The vertical axis is the ratio of the moduli of the surrounding tissue to the tube. The horizontal axis is the ratio of the tension, negative or positive, to the elasticity of the tube. Thin lines (in light red) represent the transition to an instability. The thick line (in dark green) separates stability domains of the varicose and sinuous patterns.

The drosophila tracheal system would be a good candidate to test the theory. It has been widely studied as a model of tube size regulation and the deletion of several genes causes various pathologies. Specifically, mutants lacking the Sinuous or Varicose genes display sinuous [28] and varicose morphologies [29], respectively. Although we do not have a good understanding of their roles, it is known that they are required in cell-cell junctions (associated to the rigidity of the tube) and that they have a role in controlling growth. We now show how our phase diagram could guide further experiments. The modulus of the normal tracheal wall was inferred from experiments to be around 20 kPa [30], and $\frac{h}{r_0} \approx 0.2$. Although the mechanical properties of the tracheal connective tissue have not been specifically studied, the expected order of magnitude of its modulus is $E_s \sim 100$ Pa. The relevant elastic ratio is therefore $\frac{E_s r_0^3}{E_t h^3} = 0.6 < 1$, so that sinuous instabilities are expected. Nevertheless, disturbing junctions lowers the rigidity of the tube, and a threefold decrease in E_t would favor the varicose instability. We therefore suggest that more emphasis should be put on measuring the influence of individual genes on the mechanical properties of cellular tubes.

The last situation is a tube in the absence of any dysplasia of the cell wall. The tension is then positive and we expect either a stable tube, or a classical Rayleigh-Plateau instability of an elastic cylinder. This is slightly different from the situation encountered in membrane tubes [11], since the fluid cylinder is surrounded by an elastic shell.

We study a perturbation $u_r(z) = r_0[(R_0 - 1) + C\cos(kz)]$. The situation that we wish to discuss does not involve any cell growth, and the instability thus occurs on a time scale small enough that volume conservation is a reasonable assumption. This imposes that $R_0^2 - 1 = -\frac{C^2}{2}$. Minimizing the energy with respect to C yields a finite value of A only for a tension larger than the critical value $\gamma_r = E_t h \frac{1-\nu^2}{1-q^2}$, where $q = kr_0$ (see Supplemental Material [15]). Below this critical value of the tension, the cylinder is stable. The instability occurs at the longest wavelength mode $q \to 0$. Determining the equilibrium wavelength of the pattern in the general case requires a nonlinear analysis, which is beyond the scope of this Letter. Nevertheless, if the amplitude of the perturbation approaches the radius of the tube, disconnected pearls are obtained and the most unstable wavelength can be found by studying the dynamics of the perturbation u_z. The continuity equation and a Poiseuille approximation for the flow lead at lowest order to: $\frac{\partial u_z}{\partial t} = r_0^4/(16\eta)\partial_z^2 P$, where η the fluid viscosity. The hydrostatic pressure P is calculated from the force-balance equation on the membrane $P = 1/r_0[\gamma C(-q^2 + 1) - E_t h(1 - \nu^2)C]\cos(qz/r_0)$. The most unstable wave vector is then $q_r^2 = \frac{\gamma - E_t h(1-\nu^2)}{2\gamma}$. The Rayleigh instability has been invoked to explain the sausagelike pattern observed on some arteries in Ref. [20]. It has been shown [31] that a very soft elastic cylinder can undergo a classical Rayleigh-Plateau instability. Testing the case of hollow elastic tubes in the same fashion could be an experimental confirmation to our theory. As expected, if $\gamma/E_t h \gg 1$, the most unstable wave vector converges to the wave vector of the classical Rayleigh-Plateau instability $q_{\mathrm{RP}} = \frac{1}{\sqrt{2}}$ [10].

The main result of this Letter is the stability diagram of Fig. 3 presenting the stabilities of most morphologies found in cellular tubes, depending of their mechanical properties. The buckling theory is in good quantitative agreement with the *in vivo* data. We have here deliberately used simple models for the mechanics of the tubes, to emphasize the generality of our results, and the relevance of a few dimensionless ratios to predict the observed instabilities. Most importantly, we want to stress the fact that tissue shapes could turn out to be a meaningful criterion to detect the causes of specific pathologies. For example, in the case of excretory kidney canals, dysplasia leads to a different instability than fluid accumulation. More work is clearly needed in each specific case, but we do not expect the basic physics presented in this Letter to be modified.

[1] M. Affolter, S. Bellusci, N. Itoh, B. Shilo, J.-P. Thiery, and Z. Werb, Dev. Cell **4**, 11 (2003).
[2] G. J. Beitel and M. Krasnow, Development (Cambridge, U.K.) **127**, 3271 (2000).
[3] M. A. Baer, H. Chanut-Delalande, and M. Affolter, Curr. Top. Dev. Biol. **89**, 137 (2009).
[4] D. J. Andrew and A. J. Ewald, Dev. Biol. **341**, 34 (2010).
[5] B. Lubarsky and M. A. Krasnow, Cell **112**, 19 (2003).
[6] M. Buechner, D. H. Hall, H. Bhatt, and E. M. Hedgecock, Dev. Biol. **214**, 227 (1999).
[7] B. Shraiman, Proc. Natl. Acad. Sci. U.S.A. **102**, 3318 (2005).
[8] T. Mammoto and D. E. Ingber, Development (Cambridge, U.K.) **137**, 1407 (2010).
[9] J. Ranft, M. Basan, J. Elgeti, J.-F. Joanny, J. Prost, and F. Jülicher, Proc. Natl. Acad. Sci. U.S.A. **107**, 20 863 (2010).
[10] Lord Rayleigh, Philos. Mag. **34**, 145 (1892).
[11] R. Bar-Ziv and E. Moses, Phys. Rev. Lett. **73**, 1392 (1994).
[12] S. Laurent, X. Girerd, J. J. Mourad, P. Lacolley, L. Beck, P. Boutouyrie, J. P. Mignot, and M. Safar, Arterioscler. Thromb. Vasc. Biol. **14**, 1223 (1994).
[13] S. Timoshenko and J. M. Gere, *Theory of Elastic Stability* (McGraw-Hill, New York, 1961), 2nd ed.
[14] P. Ciarletta and M. Ben Amar, J. Mech. Phys. Solids **60**, 525 (2012).
[15] See Supplemental Material at http://link.aps.org/supplemental/10.1103/PhysRevLett.109.018101 for the detailed calculation of thresholds, amplitudes, and energies of the different types of deformations.
[16] B. Peynircioglu and B. E. Cil, Cardiovasc. Intervent. Radiol. **31** (Suppl. 2), S38 (2008).
[17] P. F. J. New, AJR Am. J. Roentgenol. **97**, 488 (1966).

[18] P.-F. Plouin, J. Perdu, A. La Batide-Alanore, P. Boutouyrie, A.-P. Gimenez-Roqueplo and X. Jeunemaitre, Orphanet J. Rare Dis. **2**, 28 (2007).
[19] L. W. Welling, in *The Cystic Kidney*, edited by K. D. Gardner and J. Bernstein (Kluwer, Amsterdam, 1990), p. 99.
[20] P. Alstrøm, V. M. Eguíluz, M. Colding-Jørgensen, F. Gustafsson, and N.-H. Holstein-Rathlou, Phys. Rev. Lett. **82**, 1995 (1999).
[21] J. Yin, Z. Cao, C. Li, I. Sheinman, and X. Chen, Proc. Natl. Acad. Sci. U.S.A. **105**, 19 132 (2008).
[22] M. Basan, T. Risler, J.F. Joanny, X. SastreGarau, and J. Prost, HFSP J. **3**, 265 (2009).
[23] G. Helmlinger, F. Yuan, M. Dellian, and R. K. Jain, Nature Med. **3**, 177 (1997).
[24] A. P. Evan and J. A. McAteerin, in *The Cystic Kidney* (Ref. [19]), p. 2142.
[25] F. K. Nelson, P. S. Albert, and D. L. Riddle, J. Ultrastruct. Res. **82**, 156 (1983).
[26] E. Hannezo, J. Prost, and J. F. Joanny, Phys. Rev. Lett. **107**, 078104 (2011).
[27] R. Huang, J. Mech. Phys. Solids **53**, 63 (2005).
[28] V. M. Wu, J. Schulte, A. Hirschi, U. Tepass, and G. J. Beitel, J. Cell Biol. **164**, 313 (2004).
[29] V. M. Wu, M. H. Yu, R. Paik, S. Banerjee, Z. Liang, S. M. Paul, M. A. Bhat, and G. J. Beitel, Development (Cambridge, U.K.) **134**, 999 (2007).
[30] A. M. Cheshire, B. E. Kerman, W. R. Zipfel, A. A. Spector, and D. J. Andrew, Dev. Dyn. **237**, 2874 (2008).
[31] S. Mora, T. Phou, J.-M. Fromental, L. M. Pismen, and Y. Pomeau, Phys. Rev. Lett. **105**, 214301 (2010).
[32] P. Laprise, S. M. Paul, J. Boulanger, R. M. Robbins, G. J. Beitel, and U. Tepass, Curr. Biol. **20**, 55 (2010).